DOI: 10.1002/ejic.201100256

Synthesis and Structural Characterization of Bis(salicylaldiminato)magnesium Complexes of Varying Aggregation and Coordination State

Geoffrey T. Quinque,[a] Allen G. Oliver,[b] and Jeffrey A. Rood*[a]

Keywords: Magnesium / Salicylaldiminato ligands / Coordination number / Aggregation / X-ray diffraction

A series of salicylaldiminato ligands [$C_6H_5N{=}CHC_6H_4OH$ (^{1}L), 2,6-*i*Pr$C_6H_3N{=}CHC_6H_4OH$ (^{2}L), and 2,6-*i*Pr$C_6H_3N{=}CH$-3,5-*t*$Bu_2C_6H_2OH$ (^{3}L)] were treated with Bu_2Mg in the presence of the appropriate solvent system to yield the crystalline compounds [($^1L_6Mg_3$)·thf] (**1**), [(^2L_2Mg·thf)] (**2**), and [^3L_2Mg] (**3**). The products were characterized by ^{1}H and ^{13}C NMR spectroscopy and single-crystal X-ray diffraction. X-ray crystallographic analysis revealed that **1** adopts a unique trimeric aggregation state consisting of six-coordinate magnesium centers. Substitution of the ligand backbone resulted in the formation of the monomeric species **2** and **3**. X-ray crystallographic analyses revealed **2** as a five-coordinate, distorted square-pyramidal magnesium complex and **3** as a four-coordinate, distorted tetrahedral species. Inspection of the metrical parameters in **1**–**3** indicates a decrease in the Mg–O and Mg–N bond lengths and an increase in the N–Mg–O bite angle with a decreasing coordination number at magnesium.

Introduction

The use of chelating phenoxide Schiff-base ligands has been thoroughly investigated for use in the isolation of various coordination complexes.[1] Such ligands are useful in that they can often afford single-site complexes containing metal atoms that are stabilized by the bulk and chelating nature of the ligand.[2–4] This property is especially attractive for use with s-block metals as these are well known to form aggregates in the solid state and solution. For example, Lin and co-workers have shown that the solution behavior of magnesium alkoxide complexes supported by tridentate NNO Schiff-base ligands exist as dimers in the solid state and undergo a monomer–dimer equilibrium in solution.[3] Furthermore, Harder et al. have shown that tetradentate ligands based on bridged salicylaldimine units were effective for creating discrete, dimetallic magnesium complexes.[4]

Our interest lies in studying the effects of ligand sterics on the aggregation state of magnesium complexes. Because of the ease of steric tuning we were drawn toward the use of bidentate salicylaldiminato ligands for the isolation of homoleptic magnesium complexes. The use of such ligands has seen wide exploration in transition-metal[5] and p-block-metal chemistry.[6] For example, Darensbourg has shown that a series of bis(salicylaldiminato)zinc complexes of varying substitution predominantly exist as four-coordinate monomers.[7]

Comparatively, few studies have focused on the systematic investigation of steric effects on the structures of bis(salicylaldiminato)magnesium complexes. Bochmann and Lancaster reported a ferrocenyl-substituted (salicylaldminato)magnesium complex as an octahedral structure composed of two bidentate ligands and two THF solvent molecules.[8]

Herein, we report on a series of bis(salicylaldiminato)-magnesium complexes resulting from reaction with salicylideneaniline and substituted variants. We synthesized the substituted ligands shown in Scheme 1 according to literature procedures.[6a] It is evident from the crystal structures of the resulting magnesium complexes that the steric bulk of the ligand backbone influences not only the coordination state of magnesium, but also the aggregation state of the resulting complex.

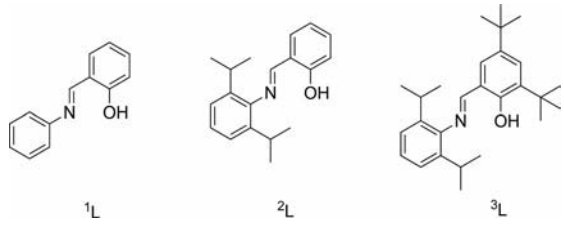

^{1}L ^{2}L ^{3}L

Scheme 1.

Results and Discussion

Complexes **1**–**3** are readily prepared by the reaction of 2 equiv. of the desired salicylaldimine with Bu_2Mg.

[a] Department of Chemistry and Biochemistry,
Elizabethtown College,
1 Alpha Drive, Elizabethtown, PA 17022, USA
Fax: +1-717-361-1394
E-mail: roodj@etown.edu
[b] Department of Chemistry and Biochemistry,
University of Notre Dame,
Notre Dame, IN 46530, USA
E-mail: aoliver2@nd.edu

Supporting information for this article is available on the WWW under http://dx.doi.org/10.1002/ejic.201100256.

Crystallization from the appropriate solvents allowed for the preparation of high-quality single crystals that were analyzed by X-ray diffraction.

Reaction of the unsubstituted ligand, salicylideneaniline (^{1}L), with Bu_2Mg resulted in the formation of a precipitate, which was dissolved at reflux in THF (Scheme 2). Slow cooling to room temperature afforded single crystals of **1** suitable for X-ray diffraction studies. The crystal structure of **1** is shown in Figure 1. This complex adopts a trimeric motif in which the three magnesium centers are bridged through the ligand oxygen atoms in a μ_2-fashion. Two different magnesium environments are present within **1**. The central magnesium atom is octahedrally coordinated to six oxygen atoms from the six salicylaldiminato ligands. Each of the two outer magnesium atoms bond to three oxygen atoms and three nitrogen atoms through chelation from three salicylaldiminato ligands. Trimeric aggregation states for magnesium complexes are somewhat rare, and this motif involving μ_2-bridging atoms is particularly unique. The closest structural analogues to **1**, which contain μ_2-O bridges, are the phosphorus-based tris(hydrazone) complexes reported by Chandrasekhar et al.[9,10] and the Schiff base complex by Dutta et al.[11] Other similar motifs involving different μ_2-bridging atoms and alkaline-earth metals include the magnesium bis(amide) [{$(Ar_FNH)_6Mg_3$·$(THF)_6$}·2tol·thf] (Ar_FNH = 2,3,4,5,6-pentafluoroaniline) by Henderson et al.,[12] the calcium arylamide [$(MesNH)_6$-Ca_3·$(THF)_6$] (Mes = 2′,4′,6′-$Me_3C_6H_2$) by Westerhausen et al.,[13] and the magnesium thiolate [$(PhS)_6Mg$·$(pyr)_6$] by Ruhlandt-Senge et al.[14]

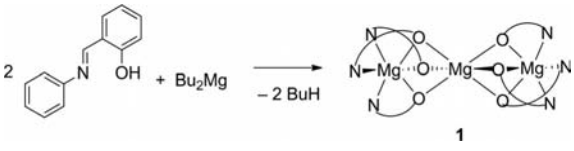

Scheme 2.

A list of selected bond lengths for **1** is shown in Table 1. Around the central atom, Mg2, the mean Mg–O bond length is 2.0729(10) Å. These bonds are slightly longer than the Mg–O bonds of the outer Mg1 and Mg3 atoms, where the mean distance is 2.0409(10) Å. Evidently, the shortening of the Mg–O bonds around these atoms results from interaction with fewer anionic oxygen atoms of the salicylaldiminate. In both cases, the remaining three coordination sites around each magnesium atom are occupied by nitrogen atoms from the imine functionality of the ligands. Here, the nitrogen atom acts as a Lewis base, donating its lone pair to the magnesium center. The average Mg–N bond length in these cases is 2.1952(12) Å. The formation and structural assignment of **1** was also confirmed through ^{1}H and ^{13}C NMR spectroscopic studies.

We were attracted to the possibility of controlling the aggregation state of the resulting complexes by varying the substituents on the salicylaldiminato ligand. We first opted to increase the steric bulk of the phenyl ring bonded to the imine nitrogen atom. Ligand ^{2}L was synthesized according

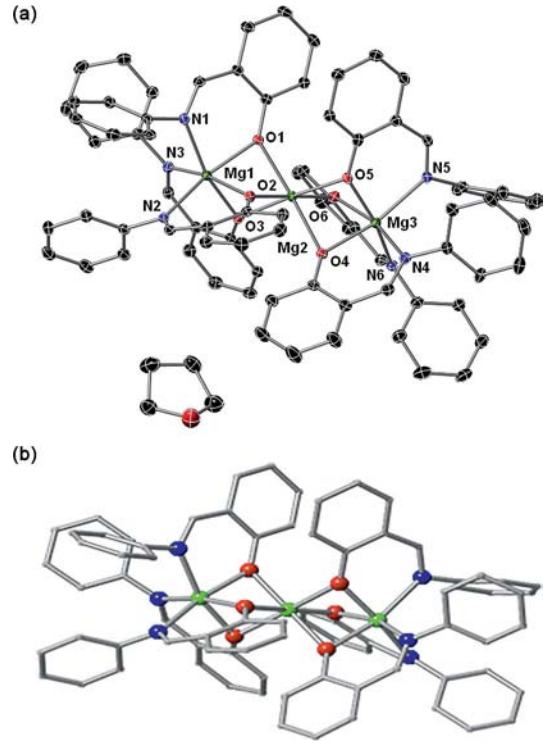

Figure 1. (a) Molecular structure of trimeric **1** with H atoms omitted for clarity. (b) Ball-and-stick model to illustrate the trimeric aggregate. Color code: Mg, green; C, black; N, blue; O, red.

Table 1. Selected bond lengths [Å] for **1**.[a]

Mg1–O3	2.0310(10)	Mg2–O5	2.0824(10)
Mg1–O2	2.0414(10)	Mg2–O4	2.0850(11)
Mg1–O1	2.0558(10)	Mg2–O1	2.1076(10)
Mg1–N1	2.1877(12)	Mg3–O5	2.0308(10)
Mg1–N2	2.1952(13)	Mg3–O4	2.0364(11)
Mg1–N3	2.2069(12)	Mg3–O6	2.0501(10)
Mg2–O2	2.0462(10)	Mg3–N5	2.1875(13)
Mg2–O6	2.0535(10)	Mg3–N6	2.1932(12)
Mg2–O3	2.0630(10)	Mg3–N4	2.2006(13)

[a] Selected bond angles for **1** may be found in the Supporting Information.

to previously reported procedures.[6a] As illustrated in Scheme 3, reaction of 2 equiv. of ^{2}L with Bu_2Mg in a hexane solution resulted in the formation of a white precipitate. Addition of THF and subsequent cooling afforded high-quality crystals.

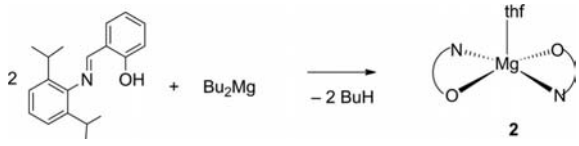

Scheme 3.

A single-crystal X-ray diffraction experiment revealed the structure of **2**, shown in Figure 2. Indeed, not only does substitution of the salicylaldiminato ligand lead to reduction in the aggregation state, but the magnesium center becomes five-coordinate in **2**. The magnesium center is co-

ordinated by two chelating salicylaldiminato ligands and a THF molecule in a distorted square-pyramidal fashion. Selected bond lengths and angles for **2** are presented in Table 2. The bond lengths between the magnesium and the salicylaldiminato oxygen atoms are 1.9368(15) and 1.9432(15) Å. These distances are much shorter than the Mg–O_{thf} bond length of 2.0433(17) Å. The coordination sphere of the central magnesium atom is completed with bonds to the imine nitrogen atoms of the salicylaldiminato ligand. Like the bond to THF, these interactions with the nitrogen atoms are Lewis acid/base in nature and exist at longer distances of 2.1500(18) and 2.1522(17) Å.

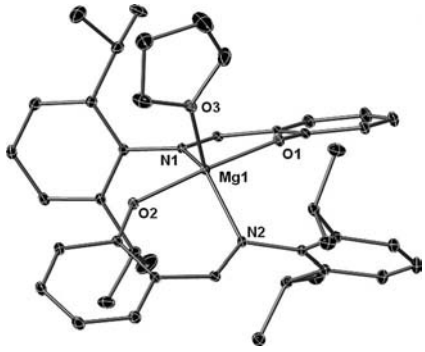

Figure 2. Molecular structure of monomeric **2** with H atoms omitted for clarity.

Table 2. Selected bond lengths [Å] and angles [°] for **2**.

Complex **2**			
Mg1–O2	1.9368(15)	O2–Mg1–N2	86.89(6)
Mg1–O1	1.9432(15)	O1–Mg1–N2	90.81(6)
Mg1–O3	2.0433(17)	O3–Mg1–N2	113.37(6)
Mg1–N2	2.1500(18)	O2–Mg1–N1	92.79(6)
Mg1–N1	2.1522(17)	O1–Mg1–N1	86.52(6)
O2–Mg1–O1	176.08(7)	O3–Mg1–N1	112.73(7)
O2–Mg1–O3	92.09(6)	N2–Mg1–N1	133.88(7)
O1–Mg1–O3	91.73(6)		

The closest structural analogue to **2** is likely to be the ferrocenyl-substituted (salicylaldiminato)magnesium complex of Lancaster and Bochmann et al., where N,O-chelation occurs at two sites around the magnesium atom. In this case, however, the magnesium atom is six-coordinate by bonding to two THF molecules.[8] It is likely that the increased steric bulk of ^{2}L prevents the octahedral geometry from occurring in **2**. Other similar five-coordinate complexes of magnesium include bis(β-diketiminato) complexes, where the fifth coordination site on the magnesium atom is occupied by a Lewis base.[15]

An ^{1}H NMR spectrum of a crystalline sample of **2** in deuterotoluene revealed an uninterpretable spectrum, possibly because of a mixture of multiple aggregates in the noncoordinating solvent. Interestingly, spiking of the deuterotoluene sample with THF simplified the spectra, suggesting that THF breaks down larger aggregates through solvation of magnesium. In accord, the ^{1}H NMR spectrum of a crystalline sample in deuteropyridine supports the structural assignment of **2** in a polar solvent. In an attempt to isolate other aggregates stemming from this behavior, crystallization experiments from noncoordinating solvents, such as toluene, were carried out. These studies consistently yielded microcrystalline powders whose ^{1}H NMR behavior mimicked that of crystalline **2** described previously.

Upon further substitution of the ligand backbone, the coordination number of magnesium decreased. Ligand ^{3}L was synthesized according to literature procedures.[6a] Reaction of 2 equiv. of ^{3}L with Bu_2Mg yielded a pale-green solution in hexane (Scheme 4). This system showed a marked increase in solubility in hexane and THF, likely resulting from the addition of bulky *tert*-butyl groups to the ligand backbone. Single crystals of **3** suitable for synchrotron X-ray diffraction were grown by vapor diffusion of acetonitrile into a hexane solution.[16]

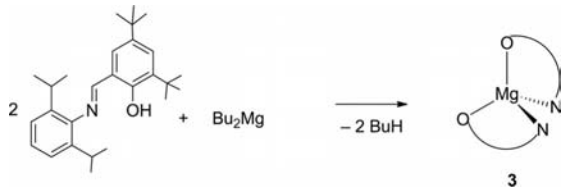

Scheme 4.

The structure of **3** contains a four-coordinate magnesium center in a distorted tetrahedral geometry. Selected bond lengths and angles found in **3** are shown in Table 3. The bonds between the magnesium centers and the anionic oxygen atoms are much shorter than the magnesium–nitrogen contacts within **3**. The bond angles indicate the distortion to a pseudo-tetrahedral geometry. ^{1}H and ^{13}C NMR spectroscopic studies support the structural assignment of **3**, (Figure 3).

Table 3. Selected bond lengths [Å] and angles [°] for **3**.

Complex **3**			
Mg1–O1	1.899(2)	O1–Mg1–O2	111.28(9)
Mg1–O2	1.8998(18)	O1–Mg1–N1	90.84(8)
Mg1–N1	2.101(2)	O2–Mg1–N1	122.01(8)
Mg1–N2	2.105(2)	O1–Mg1–N2	122.85(8)
		O2–Mg1–N2	91.34(8)
		N1–Mg1–N2	121.06(9)

Magnesium complexes containing four-coordinate centers are quite common, where alkylmagnesium, magnesium amides, and magnesium imides are only a few classifications of such cases. In terms of chelating ligands, the bulky β-diketiminato backbone has been most common in achieving low coordination states.[17] Coordination numbers of three and four for magnesium have been isolated with these ligands. Within the realm of salicylaldiminato ligands, however, the closest structural analogue to **3** is the isostructural zinc complex reported by Darensbourg and co-workers.[7] This four-coordinate species was found to be an active initiator of CO_2/epoxide copolymerization.

In comparing compounds **1**–**3**, a clear shortening of the Mg–O and Mg–N bond lengths occurs in conjunction with reduction in the coordination number of magnesium. Ac-

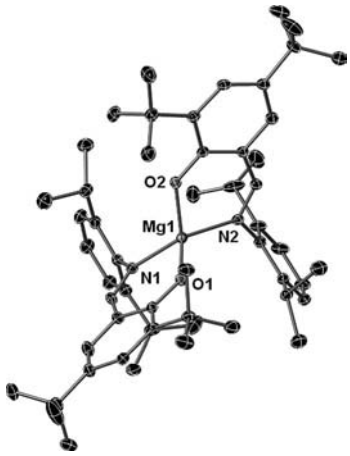

Figure 3. Molecular structure of monomeric **3** with H atoms omitted for clarity.

cordingly, the N–Mg–O bite angles increase with diminishing coordination number, indicating that the magnesium center is pulled into the binding pocket of the ligand, more so when the coordination number is decreased. Interestingly, closer inspection of the ligand backbone in **1**–**3** reveals that the C_{imine}–C_{phenyl} and N_{imine}–C_{phenyl} bonds are shorter than expected, likely indicating a degree of conjugation in each species. Conjugation in the ligand backbone could provide further attraction for the movement of the magnesium center into the binding pocket as the coordination number is lowered. The mean C_{imine}–C_{phenyl} and N_{imine}–C_{phenyl} bond lengths and the mean N–Mg–O bite angles for **1**–**3** are summarized in Table 4. Similar observations for conjugation in salicylaldiminato ligands have been noted for closely related zinc complexes.[7]

Table 4. Metrical data pertinent to magnesium–ligand binding.[a]

Complex	N–Mg–O bite angle [°]	C_{imine}–C_{phenyl} [Å]	N_{imine}–C_{phenyl} [Å]
1	84.86(5)	1.443(2)	1.439(2)
2	86.71(6)	1.443(2)	1.446(2)
3	91.09(8)	1.429(3)	1.454(3)

[a] Mean angles and distances reported.

Conclusions

Our studies illustrate that the resulting aggregation state of the bis(salicylaldiminato)magnesium product and the coordination environment around the magnesium center depend on the local steric environment of the ligand. Future studies aim at investigating the utility of **1**–**3** in performing copolymerizations of cyclic ethers and CO_2. The steric tunability of salicylaldiminato ligands makes them attractive candidates in the design of discrete metal complexes for initiating ring-opening polymerization of cyclic ethers. Complex **2** is of particular interest in that it contains a THF molecule in a potentially hemi-labile site where a cyclic ether molecule might bind. This is attractive when considering a coordination/insertion mechanism for ring-opening polymerization in conjunction with CO_2 insertion to form polycarbonates.

Although much interest has been given to CO_2 copolymerization reactions in recent times, very few examples exist of CO_2 insertion into magnesium complexes. Specifically, CO_2 has been shown to insert into Mg–N bonds to form carbamates[18] and a recent study by Ding and co-workers has illustrated the use of dimetallic magnesium complexes for the copolymerization of CO_2 and cyclohexane oxide under ambient conditions.[19] Magnesium is attractive for carrying out such processes because it is a hard Lewis acid and is oxophilic.

Experimental Section

General: All experimental manipulations were performed under an inert gas by using standard Schlenk techniques. *n*-Hexane and acetonitrile were dried with CaH_2 and distilled onto molecular sieves (4 Å) prior to use. Toluene and THF were purified by passage through a solvent purification system (LC Technology Solutions). Bu_2Mg was supplied as a 1.0 M solution in heptanes from Aldrich and was standardized prior to use. Salicylideneaniline (^{1}L) was purchased from Aldrich and recrystallized from toluene prior to use. Ligands ^{2}L and ^{3}L were synthesized from literature procedures.[6a] NMR spectra were recorded with a Varian 400MR spectrometer at 293 K. ^{1}H and ^{13}C NMR spectra were referenced internally to the residual signals of the deuterated solvent. FTIR spectra were obtained as Nujol mulls with a Nicolet Magna 760 FTIR spectrometer in the range 4000–650 cm^{-1}.

[(^{1}L$_6$Mg$_3$)·thf] (1): Bu_2Mg (1 mmol of a 1.0 M solution in heptane) was added dropwise from a syringe to a light yellow solution of salicylideneaniline (0.39 g, 2 mmol) in hexane (6 mL). An off-white precipitate formed. The reaction mixture was stirred for 2 h. THF (6 mL) was added at reflux to produce a deep-red solution. The hot solution was cooled slowly in a hot water bath to yield a small batch of clear, colorless crystals. Further cooling in a –20 °C freezer led to a larger crop of crystals. Yield 0.212 g (48%). ^{1}H NMR (400 MHz, [D$_8$]toluene): δ = 1.449 (br., 4 H, CH_2-thf), 3.549 (br., 4 H, OCH_2-thf), 6.088 (d, 12 H, aryl), 6.341 (t, 6 H, aryl), 6.743 (t, 6 H, aryl), 6.812 (d, 6 H, aryl), 6.847–6.943 (m, 18 H, aryl), 7.324 (d, 6 H, aryl), d 7.654 (s, 6 H, imine-H) ppm. ^{13}C NMR (100.5 MHz, [D$_8$]toluene): δ = 114.468, 120.18, 123.118, 123.389, 134.494, 134.951, 137.065, 154.327 (s, aryl-C), 167.469 (s, imine-C), 171.906 (s, phenolic *ipso*-C) ppm. IR: $\tilde{\nu}$ = 3059 (w), 3025 (w), 2894 (w), 1612 (s), 1590 (s), 1541 (s), 1473 (s), 1446 (m), 1397 (m), 1179 (m), 1151 (m), 1125 (m), 1032 (w), 988 (w), 850 (w), 797 (w), 753 (m), 700 (m), 595 (w), 535 (w), 498 (w) cm^{-1}. $C_{82}H_{68}Mg_3N_6O_7$ (1322.39): calcd. C 74.39, H 5.27, N 6.42; found C 74.48, H 5.18, N 6.36.

[(^{2}L$_2$Mg·thf)] (2): Bu_2Mg (1 mmol of a 1.0 M solution in heptane) was added dropwise from a syringe to a light-green solution of *N*-(2,6-diisopropylphenyl)salicylaldimine (0.56 g, 2 mmol) in hexane (7 mL) to produce an orange-red color and a small amount of white precipitate. The mixture was flash-frozen in a dry ice/acetone bath to increase the amount of white precipitate. After the solution returned to room temperature three drops of THF were added, which resulted in the formation of an orange solution. Cooling in a –20 °C freezer led to the formation of clear, pale-yellow crystals. Yield 0.270 g (41%). ^{1}H NMR (400 MHz, [D$_5$]pyridine): δ = 0.949 [d, 24 H, $CH(CH_3)_2$], 1.598 (br., 4 H, CH_2-thf), 2.942 [sept, 4 H,

C*H*$(CH_3)_2$], 3.638 (br., 4 H, OCH_2-thf), 6.316 (d, 2 H, aryl), 6.561 (t, 2 H, aryl), 7.218 (d, 4 H, aryl), 7.316 (d, 4 H, aryl), 8.279 (s, 2 H, imine-H) ppm. ^{13}C NMR (100.5 MHz, [D_5]pyridine): δ = 27.416, 24.373 [CH(CH_3)$_2$], 66.400 [s, *C*H$(CH_3)_2$], 11.580, 119.347, 124.752, 133.047, 133.395, 139.257 (s, aryl), 170.087 (s, phenolic *ipso*-C), 171.388 (s, imine-C) ppm. IR: $\tilde{\nu}$ = 3061 (w), 2961 (m), 2868 (w), 1612 (s), 1587 (m), 1531 (m), 1508 (w), 1473 (s), 1384 (m), 1362 (m), 1328 (m), 1171 (m), 1145 (m), 1108 (w), 1023 (w), 850 (w), 790 (w), 753 (m), 691 (w), 596 (w), 532 (w) cm^{-1}. Elemental analysis proved consistently problematic for **2** because of its hygroscopic nature. Originally, conflict in elemental analyses was thought to be due to a possible mixture of aggregates, as described previously by ^{1}H NMR spectroscopic studies. This, however, would likely lead to an erroneously high carbon analysis when assuming that loss of coordinated THF is involved in the formation of higher-ordered aggregates of **2**. $C_{42}H_{52}MgN_2O_3$ (657.17): calcd. C 76.76, H 7.97, N 4.26; found C 71.98, H 7.92, N 3.63.

[^{3}L$_2$Mg] (3): Bu_2Mg (1 mmol of a 1.0 M solution in heptane) was added dropwise from a syringe to a light-green solution of 3,5-di-*tert*-butyl-*N*-(2,6-diisopropylphenyl)salicylaldimine (0.47 g, 1 mmol) in hexane (7 mL). A pale-green solution resulted. Vapor diffusion with acetonitrile in a nitrogen-filled glovebox was used to facilitate the growth of small, clear, colorless crystals. Yield 0.541 g (67%). ^{1}H NMR (400 MHz, [D_8]toluene): δ = 0.958 [d, 12 H, CH(C*H*$_3$)$_2$], 1.157 [d, 12 H, CH(C*H*$_3$)$_2$], 1.206 [s, 18 H, C(CH_3)$_3$], 1.597 [s, 18 H, C(CH_3)$_3$], 2.601 [sept, 2 H, C*H*$(CH_3)_2$], 3.657 [sept, 2 H, C*H*$(CH_3)_2$], 6.871 (d, 2 H, aryl), 6.890–7.035 (m, 4 H, aryl), 7.658 (d, 2 H, aryl), 7.968(s, 2 H, imine-H) ppm. ^{13}C NMR (100.5 MHz, [D_8]toluene): δ = 22.940, 23.691, 24.985, 28.632, 28.756 [s, CH(CH_3)$_2$], 30.010, 31.459 [s, C(*C*H$_3$)$_3$], 33.960, 35.819 [s, *C*(CH_3)$_3$], 119.362, 123.970, 126.742, 130.421, 131.544, 135.811, 141.526, 141.700, 148.020 (s, aryl), 169.745 (s, phenolic *ipso*-C), 179.443 (s, imine-C) ppm. IR: $\tilde{\nu}$ = 2960 (s), 2868 (w), 1613 (s), 1578 (s), 1531 (s), 1464 (m), 1432 (s), 1405 (m), 1361 (m), 1331 (w), 1256 (m), 1232 (w), 1201 (w), 1163 (s), 1137 (w), 1098 (w), 873 (w), 839 (w), 800 (w), 765 (m), 722 (w), 573 (w), 541 (w) cm^{-1}. $C_{54}H_{76}MgN_2O_2$ (809.48): calcd. C 79.98, H 9.53, N 3.46; found C 80.12, H 9.46, N 3.46.

X-ray Crystallography: For compounds **1** and **2**, single crystals were examined under Infineum V8512 oil. The datum crystal was affixed to a thin glass fiber atop a tapered copper mounting pin and transferred to the nitrogen stream of a Bruker APEX II diffractometer equipped with an Oxford Cryosystems 700 series low-temperature apparatus. Cell parameters were determined by using reflections harvested from three sets of 12 0.5° ϕ-scans. The orientation matrix derived from this was transferred to COSMO[20] to determine the optimum data collection strategy requiring a minimum of fourfold redundancy. Cell parameters were refined by using reflections harvested from the data collection with $I \geq 10\sigma(I)$. All data were corrected for Lorentz and polarization effects, and runs were scaled by using SADABS.[21] The structures were solved from partial data sets by using the Autostructure option within APEX 2.[22] This option employs an iterative application of the direct methods, Patterson synthesis, and dual-space routines of SHELXTL.[23] Hydrogen atoms were placed at calculated geometries and allowed to ride on the position of the parent atom. Hydrogen thermal parameters were set to 1.2 times the equivalent isotropic *U* value of the parent atom. For compound **3**, intensity data were collected at 150 K with a D8 goniostat equipped with a Bruker APEXII CCD detector at Beamline 11.3.1 at the Advanced Light Source (Lawrence Berkeley National Laboratory) by using synchrotron radiation tuned to λ = 0.7749 Å. A series of 2 s frames measured at 0.3° increments of ω were collected to calculate a unit cell. For data collection, frames were measured for a duration of 2 s at 0.3° intervals of ω with a maximum 2θ value of ca. 60°. The data frames were collected by using the program APEX2 and processed by using the program SAINT routine within APEX2. The data were corrected for absorption and beam corrections based on the multi-scan technique as implemented in the SADABS program. The structures were solved from partial data sets by using the Autostructure option in

Table 5. Crystallographic data for compounds **1**–**3**.

	1	**2**	**3**
Empirical formula	$C_{82}H_{68}Mg_3N_6O_7$	$C_{42}H_{52}MgN_2O_3$	$C_{54}H_{76}MgN_2O_2$
M_r [g mol^{-1}]	1322.39	657.17	809.48
T [K]	100(2)	150(2)	296(2)
Crystal system	monoclinic	monoclinic	monoclinic
Space group	$P2_1/c$	$P2_1/n$	$C2/c$
a [Å]	17.0074(10)	11.713(5)	30.230(2)
b [Å]	18.0154(11)	20.074(9)	19.083(2)
c [Å]	22.7809(14)	16.621(7)	21.848(3)
α [°]	90	90	90
β [°]	93.3560(10)	105.291(6)	127.258(2)
γ [°]	90	90	90
V [Å^3]	6968.0(7)	3770(3)	10031.2(19)
Z	4	4	8
D [Mg m^{-3}]	1.069	1.158	1.072
μ (Mo-K_α) [mm^{-1}]	0.086	0.087	0.089
Crystal size [mm]	0.45 × 0.32 × 0.30	0.37 × 0.18 × 0.16	0.14 × 0.06 × 0.05
T_{max} and T_{min}	0.97 and 0.94	0.98 and 0.95	0.98 and 0.94
θ_{min} to θ_{max} [°]	2.21 to 26.26	2.40 to 25.28	2.42 to 25.68
Reflections collected	78591	45607	55219
Independent reflections	14242 [R(int) = 0.0351]	8880 [R(int) = 0.0395]	10252 [R(int) = 0.0652]
Observed reflections [$I > 2\sigma(I)$]	9983	8685	7891
Goodness-of-fit on F^2	1.049	1.037	1.043
R_1, wR_2 [$I > 2\sigma(I)$]	0.0340, 0.0837	0.0521, 0.1228	0.0659, 0.1029
R_1, wR_2 (all data)	0.0524, 0.0961	0.0811, 0.1394	0.1029, 0.1938
Largest peak/hole [e Å^{-3}]	0.24 and –0.26	0.75 and –0.66	0.71 and –0.68

APEX 2. This option employs an iterative application of the direct methods, Patterson synthesis, and dual-space routines of SHELXTL. Hydrogen atoms were placed at calculated geometries and allowed to ride on the position of the parent atom. Hydrogen thermal parameters were set to 1.2 times the equivalent isotropic *U* value of the parent atom. All crystallographic details are available in Table 5. CCDC-816332 (**1**), -816334 (**2**), and -816334 (**3**) contain the supplementary crystallographic data for this paper. These data can be obtained free of charge from The Cambridge Crystallographic Data Centre via www.ccdc.cam.ac.uk/data_request/cif.

Supporting Information (see footnote on the first page of this article): Bond angles for compound **1**.

Acknowledgments

We gratefully acknowledge Elizabethtown College and the Department of Chemistry and Biochemistry for start-up funds and support, and the National Science Foundation (grant CHE-0958425) for instrument support. Special thanks to Dr. Jeanette Krause, director of the Richard C. Elder X-ray Crystallography Facility at the University of Cincinnati for collection of synchrotron diffraction data. Samples for crystallographic analysis at the synchrotron were submitted through the SCrALS (Service Crystallography at Advanced Light Source) program. Crystallographic data were collected at the Small-Crystal Crystallography Beamline 11.3.1 at the Advanced Light Source (ALS). The ALS is supported by the U.S. Department of Energy, Office of Energy Sciences Materials Sciences Division, under contract DE-AC02-05CH11231 at Lawrence Berkeley National Laboratory.

[1] a) V. C. Gibson, S. K. Spitzmesser, *Chem. Rev.* **2003**, *103*, 283–315; b) A. R. F. Cox, V. C. Gibson, E. L. Marshall, A. J. P. White, D. Yeldon, *Dalton Trans.* **2006**, 5014–5023; c) P. A. Cameron, V. C. Gibson, C. Redshaw, J. A. Segal, A. J. P. White, D. J. Williams, *J. Chem. Soc., Dalton Trans.* **2002**, 415–422.

[2] a) M. H. Chisholm, *Pure Appl. Chem.* **2010**, *82*, 1647–1662; b) M. H. Chisholm, Z. Zhou, *J. Mater. Chem.* **2004**, *14*, 3081–3092.

[3] W. Hung, C. Lin, *Inorg. Chem.* **2009**, *48*, 728–734.

[4] a) D. F.-J. Piesik, R. Stadler, S. Range, S. Harder, *Eur. J. Inorg. Chem.* **2009**, 3569–3576; b) S. Range, D. F.-J. Piesik, S. Harder, *Eur. J. Inorg. Chem.* **2008**, 3442–3451.

[5] For selected examples, see: a) J. L. van Wyk, S. Mapolie, A. Lennartson, M. Hakansson, S. Jagner, *Z. Naturforsch., B* **2007**, *62*, 331–338; b) A. Pärssinen, T. Luhtanen, M. Klinga, T. Pakkanen, M. Leskelä, T. Repo, *Organometallics* **2007**, *26*, 3690–3698; c) A. Pärssinen, T. Luhtanen, M. Klinga, T. Pakkanen, M. Leskelä, T. Repo, *Eur. J. Inorg. Chem.* **2005**, 2100–2109; d) T. R. Younkin, E. F. Connor, J. I. Henderson, S. K. Friedrich, R. H. Grubbs, D. A. Bansleben, *Science* **2000**, *287*, 460–462; e) F. M. Bauers, S. Mecking, *Angew. Chem.* **2001**, *113*, 3112; *Angew. Chem. Int. Ed.* **2001**, *40*, 3020–3022; f) B.-Y. Lee, G. C. Bazan, J. Vela, Z. J. A. Komon, X. Bu, *J. Am. Chem. Soc.* **2001**, *123*, 5352–5353.

[6] For selected examples, see: a) P. A. Cameron, V. C. Gibson, C. Redshaw, J. A. Segal, G. A. Solan, A. J. P. White, D. J. Williams, *J. Chem. Soc., Dalton Trans.* **2001**, 1472–1476; b) J. Liu, N. Iwasa, K. Nomura, *Dalton Trans.* **2008**, 3978–3988; c) A. K. Jain, A. Gupta, R. Bohra, I.-P. Lorenz, P. Mayer, *Polyhedron* **2006**, *25*, 654; d) N. Sharma, A. K. Jain, R. K. Sharma, R. Bohra, J. E. Drake, M. B. Hursthouse, M. E. Light, *Polyhedron* **2003**, *22*, 2943–2952; e) J. Lewiński, J. Zachara, K. B. Starowieyski, Z. Ochal, I. Justyniak, T. Kopeć, P. Stolarzewicz, M. Dranka, *Organometallics* **2003**, *22*, 3773–3780; f) D. Pappalardo, C. Tedesco, C. Pellecchia, *Eur. J. Inorg. Chem.* **2002**, 621–628.

[7] D. J. Darensbourg, P. Rainey, J. Yarbrough, *Inorg. Chem.* **2001**, *40*, 986–993.

[8] R. K. J. Bott, M. Schormann, D. L. Hughes, S. J. Lancaster, M. Bochmann, *Polyhedron* **2006**, *25*, 387–396.

[9] a) V. Chandrasekhar, R. Azhakar, B. G. T. S. Andavan, V. Krishnan, S. Zacchini, J. F. Bickley, A. Steiner, R. J. Butcher, P. Kogerler, *Inorg. Chem.* **2003**, *42*, 5989–5998; b) V. Chandrasekhar, R. Azhakar, J. F. Bickley, A. Steiner, *Chem. Commun.* **2005**, 459–461.

[10] V. Chandrasekhar, R. Azhakar, B. Murugesapandian, T. Senapati, P. Bag, M. D. Pandey, S. K. Maurya, D. Goswami, *Inorg. Chem.* **2010**, *49*, 4008–4016.

[11] S. Dutta, P. Biswas, U. Florke, K. Nag, *Inorg. Chem.* **2010**, *49*, 7382–7400.

[12] J. A. Rood, S. E. Hinman, B. C. Noll, K. W. Henderson, *Eur. J. Inorg. Chem.* **2008**, 3935–3942.

[13] M. Gartner, H. Gorls, M. Westerhausen, *Dalton Trans.* **2008**, *12*, 1574–1582.

[14] S. Chadwich, U. Englich, M. O. Senge, B. C. Noll, K. Ruhlandt-Senge, *Organometallics* **1998**, *17*, 3077–3086.

[15] W.-Y. Lee, H.-H. Hsieh, C.-C. Hsieh, H. M. Lee, G.-H. Lee, J.-H. Huang, T.-C. Wu, S.-H. Chuang, *J. Organomet. Chem.* **2007**, *692*, 1131–1137.

[16] Crystallographic data were collected through the SCrALS (Service Crystallography at Advanced Light Source) program at the Small-Crystal Crystallography Beamline 11.3.1 at the Advanced Light Source (ALS), Lawrence Berkeley National Laboratory. The ALS is supported by the U. S. Department of Energy, Office of Energy Sciences Materials Sciences Division, under contract DE-AC02-05CH11231.

[17] a) B. M. Chamberlain, M. Cheng, D. R. Moore, T. M. Ovitt, E. B. Lobkovsky, G. W. Coates, *J. Am. Chem. Soc.* **2001**, *123*, 3229–3238; b) M. H. Chisholm, K. Phomphrai, *Inorg. Chim. Acta* **2003**, *350*, 121–125; c) M. H. Chisholm, J. C. Huffman, K. Phomphrai, *J. Chem. Soc., Dalton Trans.* **2001**, 222–224; d) B. Sedai, M. J. Heeg, C. H. Winter, *J. Organomet. Chem.* **2008**, *693*, 3495–3503; e) A. P. Dove, V. C. Gibson, P. Hormnirun, E. L. Marshall, J. A. Segal, A. J. P. White, D. J. Williams, *Dalton Trans.* **2003**, 3088–3097; f) J. L. Sebestl, T. T. Nadasdi, M. J. Heeg, C. H. Winter, *Inorg. Chem.* **1998**, *37*, 1291.

[18] a) Y. Tang, L. N. Zakharov, A. L. Rheingold, R. A. Kemp, *Organometallics* **2004**, *23*, 4788–4791; b) K. Yang, C. Chang, C. Yeh, G. Lee, Y. Wang, *Organometallics* **2002**, *21*, 1296–1299; c) K. Yang, C. Chang, C. Yeh, G. Lee, S. Peng, *Organometallics* **2001**, *20*, 126–137; d) C. Chang, B. Srinivas, M. Wu, W. Chiang, M. Y. Chiang, C. Hsiung, *Organometallics* **1995**, *14*, 5159.

[19] Y. Xiao, Z. Wang, K. Ding, *Macromolecules* **2006**, *39*, 128–137.

[20] *COSMO*, Bruker–Nonius AXS, Madison, Wisconsin, USA, **2005**.

[21] G. M. Sheldrick, *SADABS*, Bruker–Nonius AXS, Madison,-Wisconsin, USA, **2004**.

[22] APEX2 v2010.3.0 and SAINT v7.60A data collection and data processing programs, respectively, Bruker Analytical X-ray Instruments, Inc., Madison, WI; SADABS v2008/1 semi-empirical absorption and beam correction program; G. M. Sheldrick, University of Göttingen, Germany.

[23] G. M. Sheldrick, *Acta Crystallogr., Sect. A* **2008**, *64*, 112–122.

Received: March 15, 2011
Published Online: June 29, 2011

